doi:10.1246/cl.2012.62

Published on the web December 24, 2011

End-tether Structure of DNA Alters Electron-transfer Pathway of Redox-labeled Oligo-DNA Duplex at Electrode Surface

Yasuhiro Mie, Naoshi Kojima, Keiko Kowata, and Yasuo Komatsu*
Bioproduction Research Institute, National Institute of Advanced Industrial Science and Technology (AIST), 2-17-2-1 Tsukisamu-higashi, Toyohira, Sapporo, Hokkaido 062-8517

(Received October 11, 2011; CL-110828; E-mail: komatsu-Yasuo@aist.go.jp)

We prepared Nile Blue (NB)-modified 17-mer DNA duplexes with thiol/disulfide end tethers for immobilization onto gold electrodes to understand the effect of the tether structure of DNA on its electron-transfer (ET) reactions. The longer thiol tether allowed electron transfer between the NB and the electrode through the DNA duplex, whereas the direct ET pathway became predominant in the shorter disulfide tether. Importantly, the insertion of a spacer chain into the disulfide tether changed the direct ET pathway to a through-DNA pathway.

Understanding the electron-transfer (ET) reaction between a redox marker bound to a DNA molecule (redox DNA) and an electrode is essential for DNA-based devices such as electrochemical DNA/protein sensors, which enable cost-effective DNA/protein evaluations.[1–9] The ET reactions of redox-DNA have been investigated using oligodeoxynucleotides with a redox marker at one end and a tether at the other end in order to immobilize them onto the electrode surface. With respect to the ET mechanism, DNA-mediated (through the base π stack) ET between a redox marker and an electrode has been reported using intercalators as redox markers, e.g., Nile Blue (NB).[1,2,9] On the other hand, a direct ET mechanism between the two was also reported using redox markers, e.g., ferrocene (Fc) derivatives, that were pendant to the DNA strand.[3–6]

In general, alkanethiol derivatives such as a six-carbon (C6) alkanethiol (Figure 1a) have been utilized as an end tether of DNA for immobilization onto gold electrode surfaces. Recently, cyclic disulfide tethers (Figure 1b) have attracted much attention because of their more stable attachment of the DNA strand onto electrode surfaces.[10–12] As compared to typical C6 thiol tethers, disulfide tethers have a much shorter and a more rigid spacer between the DNA terminal and the sulfur atom that binds to the electrode surface (Figure 1). Although the effect of a short tether structure has been reported using a C2 alkanethiol of Fc-pendant DNA with a direct ET pathway,[3] the effects of the disulfide tether and a short tether with marker-intercalated DNA have remained poorly understood. Clarifying this point is important to yield useful information for understanding the ET reactions of redox DNA in order to construct more efficient DNA-based electrochemical devices. In this context, we prepared NB-modified 17-mer DNA with the tether of C6 thiol, cyclic disulfide, or cyclic disulfide containing a triethylene glycol chain (Figure 1; C6S-tether, SS-tether, and SS-EG_3-tether) and compared their ET reactions at gold surfaces. Herein we report our finding that the ET pathway between an electrode and a redox marker in a DNA strand can be changed by varying the end-tether structure of the DNA.

Oligonucleotides were prepared on a solid support by using standard phosphoramidite chemistry.[13] A thiol- or cyclic disulfide tether was introduced at the 5′-terminus of the DNA strand using the C6 S–S or dithiol phosphoramidite (DTPA) modifier (Glen Research, Sterling, VA), and a triethylene glycol chain was introduced into the DNA using the spacer phosphoramidite 9 (Glen Research). Modification by the NB at the 5′-terminus of the DNA was carried out according to a published method.[9] Complementary DNA sequences included tether-5′-GA–GAT–ATA–AAG–CAC–GCA-3′ and NB–5′-UGC–GTG–CTT–TAT–ATC–TC-3′.

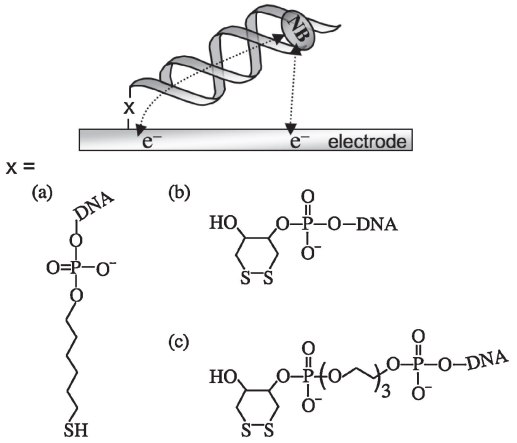

Figure 1. Schematic representation of the electrode reaction of redox DNA and structures of the end tethers of DNA used in this study: (a) C6 alkanethiol tether, (b) cyclic disulfide tether, and (c) cyclic disulfide tether modified with a triethylene glycol spacer.

Gold disk electrodes ($\phi = 3$ mm, Bioanalytical Systems, West Lafayette, IN) were cleaned according to previously reported methods.[14,15] In the present study, the polycrystalline gold electrode was chosen in a practical sense. DNA immobilization was performed by placing a 10 μM tether–DNA–NB solution on the electrode surface for 17 h. The prepared surface was backfilled with sulfanylhexanol according to a reported procedure.[5] Voltammetry was performed with a normal three-electrode configuration consisting of a Ag/AgCl reference electrode, a Pt auxiliary electrode, and a DNA-modified working electrode, typically in a 5 mM phosphate buffer (pH 7) containing 50 mM NaCl. For the kinetic analysis, experimental data were collected in the log(v) region where the voltammetric behavior obeys the surface regime.

Imaging of the DNA-modified surface was performed using atomic force microscopy (AFM, SPI3700, Seiko Instruments, Tokyo) under ambient conditions in the dynamic force mode with silicon cantilever-based tips (Seiko Instruments). The cantilevers had a nominal spring constant of 2 N m^{-1}. DNA

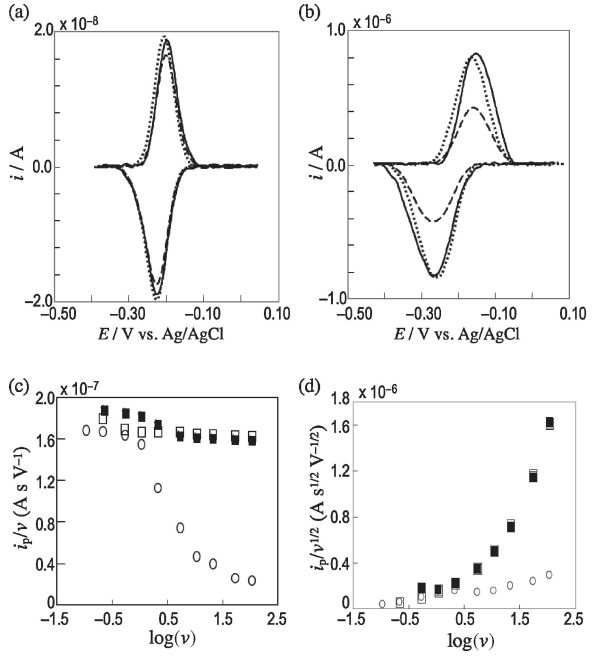

Figure 2. Cyclic voltammograms of C6S–DNA–NB (solid line), SS–DNA–NB (dashed line), and SS–EG_3–DNA–NB (dotted line) modified gold electrodes in 5 mM NaPi (pH 7.1) containing 50 mM NaCl measured at scan rates of (a) 0.1 and (b) 5 V s^{-1}, and scan rate (v) dependence of the currents (i_p) in voltammograms obtained from the electrodes modified with C6S–DNA–NB (filled square symbols), SS–DNA–NB (opened circle symbols), and SS–EG_3–DNA–NB (opened square symbols). (c) Peak current function of i_p/v versus log(v). (d) Peak current function of $i_p/\sqrt{v}$ versus log(v).

films were prepared on a gold/mica surface (Agilent Technologies, Santa Clara, CA).

First, we performed cyclic voltammetry of both C6–DNA–NB and SS–DNA–NB films. Figures 2a and 2b show baseline-corrected voltammograms measured at lower (0.1 V s^{-1}) and higher (5 V s^{-1}) potential scan rates. Both DNA electrodes displayed a couple of peaks at −0.19 V (vs. Ag/AgCl), and the formal potential was consistent with the reported value for NB intercalated in DNA,[1] supporting an ET between the NB in the DNA and the electrode. At a scan rate of 0.1 V s^{-1}, the anodic and cathodic peak currents (i_{pa} and i_{pc}, respectively) of both DNA films were of similar magnitude under the present conditions. The amount of DNA molecules on the surface, estimated by charges passed through in the voltammograms, were about 3.0 (±0.5) and 2.7 (±0.5) pmol cm^{-2} for C6–DNA–NB and SS–DNA–NB, respectively. These values were quite similar to those (ca. 2–5 pmol cm^{-2}) reported for 17-mer NB-modified DNA[1] and 20-mer Fc-modified DNA.[3] Interestingly, at the higher scan rate (5 V s^{-1}), the current of SS–DNA–NB was about half that of C6–DNA–NB.

The relationship between the peak currents (i_{pc}) obtained from the voltammograms against the scan rates (v) is shown in Figures 2c and 2d. In the case of C6S–DNA–NB, the ratio of the peak currents over the scan rates, i_p/v, remained almost constant against log(v), exhibiting Nernstian behavior characteristics of a surface-confined redox species. On the other hand, the i_p/v values of SS–DNA–NB decreased dramatically with increasing log(v) at a certain point. These results suggest that C6S–DNA–NB and SS–DNA–NB films have different mechanisms of ET between the NB and the electrode. Slinker et al. proved ET through a DNA duplex (π stacks) between NB and an electrode,[1] and we used the same sequences and tether structure for C6–DNA–NB. Furthermore, it is reasonable to hypothesize that when the ET occurred through the π stacks, the i_p/v values were independent of v. Hence, we could confirm that DNA-mediated ET occurred at the C6S–DNA–NB-modified electrode. In the case of SS–DNA–NB, since the i_p/v values were strongly dependent on v, a DNA-mediated ET mechanism would not fit the case. Anne et al. and Ikeda et al. demonstrated a direct ET mechanism using Fc pendant ca. 20-mer DNA duplexes.[3,5] With the direct ET mechanism, it is concluded that the i_p/v values decrease drastically at higher log(v) because of the elastic diffusion of the redox marker resulting from bending of the DNA duplex to contact the electrode surface required for the ET to take place. In such a case, the plots for the values of the peak currents over the square root of the scan rate, $i_p/\sqrt{v}$, against log(v) exhibit bell-shaped profiles. Although the $i_p/\sqrt{v}$ values of C6S–DNA–NB increased with increasing log(v), SS–DNA–NB exhibited a profile close to the bell-shape (Figure 2d), indicating the direct ET mechanism.

To further understand the effects of the tether structure, we next conducted an ET analysis of SS–EG_3–DNA–NB. The voltammograms revealed a couple of peaks corresponding to the NB redox reaction (Figures 2a and 2b). The scan rate dependence of these voltammetric currents together with the C6–DNA–NB and SS–DNA–NB is shown in Figures 2c and 2d. The i_p/v remained almost constant against log(v), whereas the $i_p/\sqrt{v}$ increased with increasing log(v). These characteristics are very similar to those of the C6S–DNA–NB-modified electrode and are significantly different from those of SS–DNA–NB. These results suggest that electrons were transferred through the DNA duplex at SS–EG_3–DNA–NB-modified electrode and that the introduction of a longer spacer into the SS-tether changed its ET mechanism from direct ET to DNA-mediated ET. The ET rate constant (k_s) obtained for SS–EG_3–DNA–NB from the voltammetric peak positions against log(v) according to Laviron's treatment[16] was 14 s^{-1}. This was very close to the reported value (12 s^{-1}) of the DNA-mediated ET mechanism for a daunomycin-intercalated DNA film,[17] which has a tether length similar to that of SS–EG_3. If ET occurred with a DNA-mediated mechanism for both SS– and SS–EG_3–DNA–NB electrodes, then on the basis of k_s (14 s^{-1}) for SS–EG_3–DNA–NB, SS–DNA–NB should have a k_s value larger than 700 s^{-1}. This is because k_s increases exponentially with decreasing tether length in the DNA-mediated mechanism,[17] and SS–DNA–NB has a much shorter tether length than SS–EG_3–DNA–NB. However, the k_s value for SS–DNA–NB was estimated to be 41 s^{-1}, which was much smaller than that expected for DNA-mediated ET. These results again suggest that a different ET mechanism had taken place with respect to the tether length (structure) of the DNA.

Since the tether length may alter the orientation of the DNA duplex at the surface to affect ET reactions, we performed AFM measurements of the DNA films to evaluate their surface structures. The AFM images obtained for C6–, SS–, and SS–EG_3–DNA–NB-modified surfaces (Figure 3) showed spots with diameters of 10–20 nm, as described in previous reports of DNA

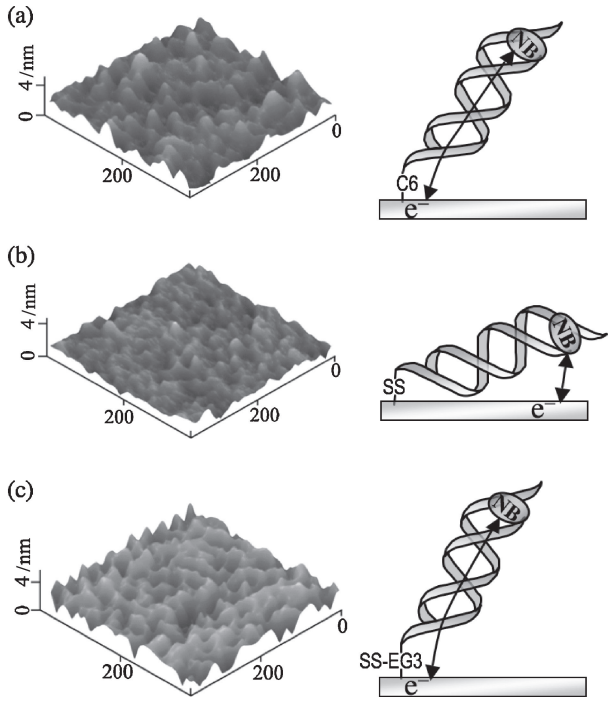

Figure 3. AFM images of (a) C6S–DNA–NB-, (b) SS–DNA–NB-, and (c) SS–EG_3–DNA–NB-immobilized gold surfaces and a schematic representation of the "upright" and "lie-down" orientations of these oligo-DNAs at an electrode surface. Arrows denote the dominant ET pathways.

films,[18–21] indicating that each spot corresponded to a DNA molecule. The maximum heights of the spots were 4.2, 2.7, and 4.7 nm for the C6S–DNA–NB, SS–DNA–NB, and SS–EG_3–DNA–NB films, respectively. Considering the lengths of the 17-mer DNA duplex and the tether, it was calculated that C6S–DNA–NB, SS–DNA–NB, and SS–EG_3–DNA–NB were oriented at angles of approximately 43, 27, and 47°, respectively, from the electrode surface. For C6–DNA–NB, the value is consistent with those (45–60°) reported for DNA with a C6 linker. These results showed different orientations of the DNA associated with the structure of the terminal tethers. In other words, the longer C6S-tether and SS–EG_3-tether could give the DNA helix an upright orientation under the present conditions, whereas the SS-tether laid the DNA down flat, almost parallel to the gold surface (Figure 3b). The motion of DNA helix with a shorter SS-tether is assumed to become more restricted upon binding to the electrode surface because of the two-point attachment of the cyclic structure with no spacer chain between the helix and the tether; thus, the tether–DNA bond seems to direct it to being close to parallel to the surface (Figure 1). Furthermore, the proximity of the DNA and the electrode surface due to the shorter tether might cause nonspecific interactions between them. Therefore, a lie-down orientation of SS–DNA–NB would be reasonable. Combined with the above electrochemical results, it can be concluded that DNA-mediated ET occurred when the DNA had an upright orientation, whereas direct ET was preferable with a lie-down orientation. Since the base π orbitals are aligned (parallel) along the helical axis, electronic coupling between the π orbitals and the electrode surface necessary for DNA-mediated ET is hindered at the SS–DNA–NB electrode because of the lie-down orientation. Hence, the SS–DNA–NB film might predominantly utilize a direct ET mechanism.

In summary, the effects of the end-tether structure of redox-DNA on its ET reactions at the electrode surface were investigated using a 17-mer DNA labeled with NB, a redox active intercalator. Three types of end tethers were introduced at the 5′ end of the complementary oligonucleotides for immobilization on the electrode surface. DNA-mediated ET between the NB and the electrode occurred when the DNA had an upright orientation with a longer C6S- or SS–EG_3-tether, whereas direct ET took place when the DNA had a lie-down orientation with a shorter SS-tether. The present results suggest that the structure of the end-tether can determine the ET pathway of redox DNA at electrode surfaces by regulating the orientations of the DNA molecules.

This study was partially supported by a Grant-in-Aid for Scientific Research (No. 23790065) from the Ministry of Education, Culture, Sports, Science and Technology, Japan.

References

1 J. D. Slinker, N. B. Muren, S. E. Renfrew, J. K. Barton, *Nat. Chem.* **2011**, *3*, 228.
2 E. L. S. Wong, J. J. Gooding, *J. Am. Chem. Soc.* **2007**, *129*, 8950.
3 A. Anne, C. Demaille, *J. Am. Chem. Soc.* **2008**, *130*, 9812.
4 F. Ricci, N. Zari, F. Caprio, S. Recine, A. Amine, D. Moscone, G. Palleschi, K. W. Plaxco, *Bioelectrochemistry* **2009**, *76*, 208.
5 R. Ikeda, S. Kitagawa, J. Chiba, M. Inouye, *Chem.—Eur. J.* **2009**, *15*, 7048.
6 S. Sato, M. Tsueda, S. Takenaka, *J. Organomet. Chem.* **2010**, *695*, 1858.
7 R. H. Liu, W. A. Coty, M. Reed, G. Gust, *IVD Technol.* **2008**, 31.
8 N. Nakamura, T. Fukuda, S. Nonen, K. Hashimoto, J. Azuma, N. Gemma, *Clin. Chim. Acta* **2010**, *411*, 568.
9 A. A. Gorodetsky, W. J. Hammond, M. G. Hill, K. Slowinski, J. K. Barton, *Langmuir* **2008**, *24*, 14282.
10 D. H. Paik, Y. Seol, W. A. Halsey, T. T. Perkins, *Nano Lett.* **2009**, *9*, 2978.
11 P. Liepold, T. Kratzmüller, N. Persike, M. Bandilla, M. Hinz, H. Wieder, H. Hillebrandt, E. Ferrer, G. Hartwich, *Anal. Bioanal. Chem.* **2008**, *391*, 1759.
12 N. L. Rosi, D. A. Giljohann, C. S. Thaxton, A. K. R. Lytton-Jean, M. S. Han, C. A. Mirkin, *Science* **2006**, *312*, 1027.
13 N. Kojima, T. Takebayashi, A. Mikami, E. Ohtsuka, Y. Komatsu, *J. Am. Chem. Soc.* **2009**, *131*, 13208.
14 Y. Mie, M. Suzuki, Y. Komatsu, *J. Am. Chem. Soc.* **2009**, *131*, 6646.
15 Y. Mie, M. Ikegami, Y. Komatsu, *Electrochem. Commun.* **2010**, *12*, 680.
16 E. Laviron, *J. Electroanal. Chem. Interfacial Electrochem.* **1979**, *101*, 19.
17 T. G. Drummond, M. G. Hill, J. K. Barton, *J. Am. Chem. Soc.* **2004**, *126*, 15010.
18 N. Mourougou-Candoni, C. Naud, F. Thibaudau, *Langmuir* **2003**, *19*, 682.
19 E. Huang, M. Satjapipat, S. Han, F. Zhou, *Langmuir* **2001**, *17*, 1215.
20 M. Sam, E. M. Boon, J. K. Barton, M. G. Hill, E. M. Spain, *Langmuir* **2001**, *17*, 5727.
21 T.-H. Nguyen, S.-M. Lee, K. Na, S. Yang, J. Kim, E.-S. Yoon, *Nanotechnology* **2010**, *21*, 075101.

